

Assessment of contour profile quality in D&B tunnelling

*Original*

Assessment of contour profile quality in D&B tunnelling / Costamagna, Elisa; Oggeri, Claudio; Ricardo, Castedo; Pablo, Segarra; Juan, Navarro. - In: TUNNELLING AND UNDERGROUND SPACE TECHNOLOGY. - ISSN 0886-7798. - STAMPA. - 75:May 2018(2018), pp. 67-80. [10.1016/j.tust.2018.02.007]

*Availability:*

This version is available at: 11583/2691975 since: 2018-02-26T12:45:25Z

*Publisher:*

elsevier

*Published*

DOI:10.1016/j.tust.2018.02.007

*Terms of use:*

This article is made available under terms and conditions as specified in the corresponding bibliographic description in the repository

*Publisher copyright*

EDP preprint/submitted version e/o postprint/Author's Accepted Manuscript

© EDP Sciences. The original publication is available at [https://authors.elsevier.com/a/1WcGp\\_KARpcRZI](https://authors.elsevier.com/a/1WcGp_KARpcRZI)

(Article begins on next page)

# 1 ASSESSMENT OF CONTOUR PROFILE QUALITY IN D&B TUNNELLING

2

3 Elisa COSTAMAGNA (\*), Claudio OGGERI (\*), Pablo SEGARRA (\*\*), Ricardo CASTEDO (\*\*), Juan  
4 NAVARRO (\*\*)

5 (\*) DIATI, Politecnico of Turin, Italy

6 (\*\*) Universidad Politécnica de Madrid, E.T.S.I. Minas y Energía, Spain

7

8

9

## 10 Abstract

11 Contour profile quality affects tunnel excavation costs, in terms of operational safety, support materials  
12 and construction time. In drill and blast tunnelling, under/over-excavation and rock mass damage arising  
13 from excavation phase can be evaluated by means of the elaboration of survey data and geophysical testing  
14 or coring, before and after the blast. As far as the quality of the profile is concerned, some indices can be  
15 used to define the contour and for the rock mass in the boundary as well.

16 This paper proposes a methodology well applicable to rock tunnelling, and a case study based analysis to  
17 correlate the over-excavation and the rock mass conditions is discussed to validate the procedure. Profiles  
18 and geological parameters have been processed with automatic code specifically developed for the study.  
19 Over-excavation distance and Tunnel Contour Quality Index are evaluated and compared with Q-system  
20 values. The results have been discussed, compared with other literature cases and validated for engineering  
21 applications.

22 **Keywords:** controlled blasting, contour evaluation, TCI, BDI, overbreak

23

## 24 1. Introduction

25 The quality of the excavated contour in underground tunnel directly affects final costs of the  
26 infrastructural facilities (*Scoble et al.*, 1997; *Hu et al.*, 2014). Poor contouring can produce under or over-  
27 excavation and artificial fractures into the rock mass. These factors produce many unfavourable  
28 consequences: scaling or specific supports are required, advancing rate decreases, convergences may  
29 increase, time schedule increases and safety is compromised. Directly related to the convergences and safety,  
30 also static approval tests are facilitated by a good contour profiling: in fact, both first phase lining and final  
31 lining are affected in terms of thickness, strength and durability (*Pelizza et al.*, 2000).

32 Rock mass conditions are an essential factor in choosing the adequate excavation method (*Mahdevari et*  
33 *al.*, 2013); drill and blast (D&B) technique is the most appropriate in rock masses that present high  
34 compressive strength and that are abrasive (*Cardu et al.*, 2004). Contour quality in D&B tunnelling depends  
35 on many factors: geological properties and conditions (e.g. rock mass quality and stress), blast design and  
36 drilling pattern execution (*Oggeri and Ova*, 2004; *Singh and Xavier*, 2004; *Singh et al.*, 2013). Initial rock  
37 mass conditions depend on the site geology, but drilling operations and blasting round affect the rock mass  
38 structure because of vibrations, shock wave propagation, gas pressure and stress redistribution (*Singh et al.*,  
39 2003; *Hu et al.*, 2014). These factors act on the rock mass depending on the microstructural fabric orientation  
40 (*Nasseri et al.*, 2011) and pre-existing fractures. Charge per delay and total charge per round must be  
41 adequately set to preserve rock mass integrity or avoid previous fractures worsening. Charge limit criteria  
42 cannot be based on the peak particle velocity (PPV) values as it happens for the man-made structures,  
43 because the limit charge is usually determined to control excessive vibration consequences at distance  
44 (*Cardu et al.*, 2004). However, even if approximated from elastic media and pure compression waves, PPV  
45 relates the acoustic impedance with the stress level that the blast produces because of rock type, stress  
46 conditions, rock properties (i.e. density, porosity, anisotropy), water content and temperature (*Singh et al.*,  
47 2003). Blast sequence directly affects the extension of induced fractures; all blasting (contour, production,  
48 smooth) in each round produce a cumulative damage effect, both with smooth blasting or pre-splitting  
49 method. However, the two methods present some differences in the orientation and intensity of the damage  
50 that they generate. The smooth blasting produces both columnar shaped elements finely spaced and also  
51 widespread micro cracks; while in the pre-splitting the formation of columnar steep elements is more  
52 extended (*Hu et al.*, 2014).

53 Taking into account the importance of the determination of rock damage and contour conditions after a  
54 D&B tunnelling, related to rock mass geology, geostructural features, drilling pattern and blasting sequence,  
55 this paper focuses on the assessment on the quality of the tunnel profile by means of some indices. This can  
56 be done using quick, easy to find and reliable profile survey techniques, properly adjusted and whose data  
57 can be processed to let a practical tool available for technical control and also to limit contractual disputes.

## 58 **2. Damage indices**

59 *Damage* in rock mass means a drop of strength, caused by the opening or shearing of new or extended  
60 cracks and joints (*Scoble et al.*, 1997). It can affect both underground and open pit excavations and it is  
61 related to the previous discontinuities conditions. The blast produces a direct damage around the blastholes  
62 and also an indirect damage due to vibration and rock block dislocation. Vibrations and explosive detonation  
63 products can propagate fractures into the rock mass and open existing joint, and this can induce an  
64 excavation disturbed zone (EDZ). This zone is the resulting volume around the tunnel boundary, whose  
65 extension depends on the excavation method, also valid for the extent of non- blasting methods (*Barton*,  
66 2007), affected by damages due to excavation and disturbance due to stress state modification. Considering  
67 underground tunnelling, the damage can be generally divided in three classes:

- 68 • Major damage: when there is rock falling from tunnel roof and/or pillar.
- 69 • Minor damage: when there is chips detachment from tunnel roof and/or pillar.
- 70 • No damage: when there is not visual damage.

71 Various techniques can be used for the rock damage evaluation, some were developed for particular  
72 studies, and others are used during excavation routine (*Scoble et al., 1997; Singh and Xavier, 2005*):

- 73 ▪ Assessing pre-blast: the inherent damage is evaluated, constructing a geomechanical  
74 classification (i.e. Bieniawski's classification) in order to build a base reference for post blast.
- 75 ▪ Visual inspection and survey: provide qualitative information on pre/post blast damage and a rock  
76 mass classification. Also a borehole camera can be used for core assessment.
- 77 ▪ Traditional observation methods: give an indirect measurement of damage. Usually the Half-Cast  
78 Factor (HCF) or scaling time is used.
- 79 ▪ Rock mass classification methods: empirical rock mass quality rating systems (e.g. Q-system),  
80 inherent-damage index and blast-induced damage (e.g. Blast Damage Factor, Blasting Damage  
81 Index).
- 82 ▪ Geophysical methods: such as seismic tomography, loose rock detection sensors and ground-  
83 penetrating radar, high-frequency cross-hole seismic, seismic-refraction tomography.
- 84 ▪ Vibration analysis: the damage in the near-field is evaluated from peak particle velocity (PPV)  
85 values and rock mass strength.

86 Four main indices are available for this evaluation: Blast Damage Factor, Blast Damage Index, Failure  
87 Approach Index and Tunnel Quality Index, that are briefly illustrated in the following sections. They do not  
88 describe the geometrical condition of the excavated contour, which depends on the comparison with the  
89 design profile, but they focus on the rock mass damage. During an underground excavation, each blast round  
90 is individually mapped, in order to evaluate or update the required support (*Barton et al., 1995*) and to  
91 modify, if necessary, drilling pattern and blast design.

92 The Q index has been the one used in this study because of the available data. Anyway, the others are  
93 presented here in order to provide a more complete overview on the available indices. These could be used in  
94 further work if the data collection will take their parameters into account.

## 95 **2.1 Blast Damage Factor**

96 The Blast Damage Factor  $D$  (*Hoek et al., 2002; Hoek, 2012*) is a parameter introduced in 2002 into the  
97 Hoek-Brown failure criterion. It estimates the global rock mass strength and the rock mass modulus. Its  
98 range falls between 0 (undisturbed rock mass) and 1 (highly disturbed rock mass). This parameter must be  
99 set only for the actual zone of damage, not for the entire rock mass surrounding the excavation and the  
100 definition of this extension represents a meaningful assessment. Ideally, the volume between front and  
101 undisturbed rock mass can be divided into a number of layer with different values of  $D$  using numerical  
102 modelling, but usually a single  $D$ -value is set for practical reasons. The production blasting data help to

103 determine the actual damaged volume; some outlines (*Hoek et al.*, 2002) suggest the right  $D$ -value by giving  
104 a description of the rock mass and its appearance. Figure 1 – 4 show some examples for D&B tunnelling  
105 (and also one example of mechanized underground excavation).

106



107

108 **Figure 1. Primolano tunnel (Italy). High quality of the tunnel contour, half blasthole clearly evident at ribs and crown.**  
109 **Suggested  $D = 0$ . (Courtesy Italesplosivi)**

110



111

112 **Figure 2. Irregular tunnel contour after D&B; shotcrete for the first phase support is smoothing asperities and over**  
113 **excavation, but nominal profile is not obtained yet. Suggested  $D = 0.7$ . (Anonymous)**

114



115

116 **Figure 3. Hydropower tunnel in Northern Italy. Local damage and irregular profile at rib is due to spalling in**  
117 **metamorphic rock mass and anisotropic state of stress, even if mechanised tunnelling with a full face open TBM has been**  
118 **adopted. Suggested  $D = 0.7$ . (Photo by C. Oggeri)**

119



120

121 **Figure 4. Very irregular profile after D&B tunnelling due to rock joint pattern and poor contouring techniques.**  
122 **Suggested  $D = 0.8$ . (Photo by C. Oggeri)**

123 **2.2 Blast Damage Index**

124 Blast Damage Index (*BDI* - Equation 1) was developed by *Yu and Vongpaisal* (1996) for mining works.  
 125 This relation takes into account the mechanics and the effects of wave propagation into the rock mass: the  
 126 compression wave arrives at the free surface and is reflected as a tensile stress wave that causes the damage  
 127 (*Barton, 2007*). They analysed how much mining work affects slope walls and roof stability. *Cardu et al.*  
 128 (2004) used this index to assess rock slope induced damage along mountainsides, when the advancing face of  
 129 a tunnel approaches the external slope.

$$130 \quad BDI = \frac{IS}{DR} = \frac{Vdc}{KT} \quad (1)$$

131 Where:

- 132 • *IS*: induced stress.
- 133 • *DR*: damage resistance.
- 134 • *V*: vector sum of PPV (mm/s).
- 135 • *d*: specific gravity for rock mass (kg/m<sup>3</sup>).
- 136 • *C*: compression wave velocity of rock mass (mm/s).
- 137 • *K*: site quality constant.
- 138 • *T*: dynamic tensile strength of rock mass (N/m<sup>2</sup>).

139 *Yu and Vongpaisal* (1996) and *Singh et al.* (2003) assume the value of *RMR* (Rock Mass Rating) as site  
 140 quality constant *K*, that is the most adopted.

141 Table 1 shows a comparison between *BDI* ranges. Mining works presents higher limits of *BDI* than  
 142 mountainside places (*Cardu et al., 2004*) but in both cases varies from zero to one. *Singh et al.* (2003)  
 143 recommended very different limits in a coal mine situation.

144 **Table 1. Comparison of *BDIs* in mining works *Yu and Vongpaisal* (1996), mountainside cases (*Cardu et al. 2004*) and coal  
 145 mine *Singh et al.* (2003).**

<i>BDI</i>	Mining	Mountainside	Coal Mine
Absolutely safe	< 0.125	< 0.060	< 1
No noticeable damage/falls seldom	< 0.250	< 0.200	< 2
Serious problems	> 0.250	> 0.200	> 2

146

### 147 2.3 Failure Approach Index

148 Failure Approach Index (*FAI*) proposes a quantification of the rock mass damage when numerical  
 149 simulations are used in tunnel support design (*Xu et al., 2017*). At the beginning it was developed for plastic  
 150 behaviour but then it was improved (*Xu et al., 2017*) for an elastic-plastic model that takes into account the  
 151 relation between stress and strain, the strength criterion and also the post-failure response, considering

152 isotropic conditions. This index is proposed for interlayered rock ( $FAI_m$ ) and bedding plane ( $FAI_j$ ) in order to  
153 find the layered rock mass FAI, which is the maximum between those two.

## 154 2.4 Q-system

155 Tunnel Quality Index (Q-system) is a consolidated and suitable rock mass classification system developed  
156 by *Barton* (1974). It is extensively used in underground rock engineering application and it allows also some  
157 correlations to empirically estimation of rock mass properties.

158 There are some parameters that need careful evaluation in order to improve the accuracy of Q-system;  
159 among the others, joint orientation is related to tunnel axis orientation but it is not numerically ranked. In fact  
160 the numerical evaluation of this parameter would make the classification less general. Moreover, joints and  
161 their characteristics are often difficult to be correctly determined: they form complicated three-dimensional  
162 patterns in the crust, while surveys are made in surfaces (two-dimensional) or boreholes (one-dimensional)  
163 (*Palmstrom*, 2005).

## 164 3. Overbreak evaluation

165 Tunnel excavation quality depends also on the contour geometry. Overbreak or bad profiling directly  
166 affects construction costs: more supports are required to avoid that some rock falls and more concrete is  
167 necessary to fill up empty spaces in order to help covering layer installation (*Scoble et al.*, 1997).  
168 Furthermore, the type and quantity of supports (preliminary and long term layer) affects static approval tests,  
169 both during construction stage and long term monitoring (*Pelizza et al.*, 1999; *Pelizza et al.*, 2000)

170 Some key indicators can be used:

- 171 1. Overbreak area (*Mahtab et al.*, 1997; *Mandal and Singh*, 2009). It is the excavated section area  
172 that exceeds the design (or paid) tunnel section. It is evaluated on a percentage on the design  
173 section area.
- 174 2. Overbreak distances (*Kim*, 2009; *Olsson*, 2010). It is the distance between design and excavated  
175 contour.
- 176 3. Tunnel Contour Quality Index (*Kim*, 2009; *Kim and Bruland*, 2010; *Kim and Bruland*, 2015).  
177 This index relates overbreak distances, contours ratio and longitudinal variation in each blasted  
178 round. It can also be evaluated for the entire tunnel.

### 179 3.1 Overbreak area indicator

180 The magnitude of overbreak can be defined as the difference between design and excavated sections. It  
181 allows to evaluate the volume of rock that exceeds the planned mucking. In order to consider comparable  
182 data, the overbreak area ( $O_{v\ area}$ ) is evaluated in percentage (*Mahtab et al.*, 1997; *Mandal and Singh*, 2009) as  
183 the difference between excavated ( $A_e$ ) and design ( $A_d$ ) tunnel section, normalized on the design section area  
184 (Equation 2):



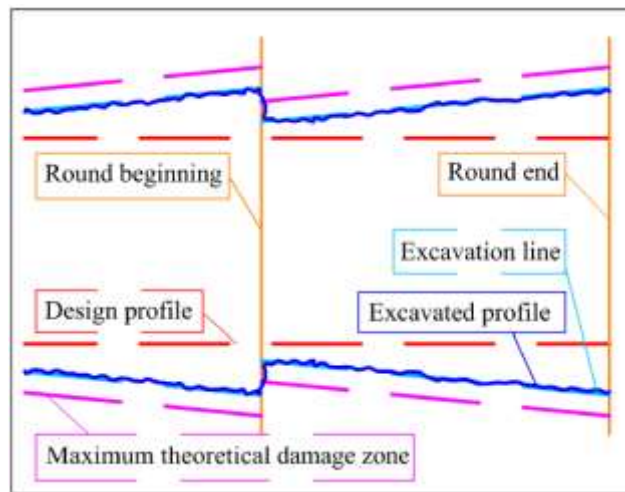
185 
$$O_{v\text{area}} = \frac{A_e - A_d}{A_d} \times 100 \quad (2)$$

186 *Mandal and Singh* (2009) also propose to divide the cross-section in three zones, in order to evaluate the  
 187 impact of different stress path and blast design effects. This approach demonstrates that the crown is more  
 188 affected by overbreak, due to its stress conditions, claiming for a particular attention on the drill plan and the  
 189 blast design of this zone.

190 **3.2 Overbreak distances and damage distances indicator**

191 In construction manual guidelines and contractual claim, the overbreak is generally evaluated as the  
 192 distance between design and excavated contour (*Mahtab et al.*, 1997; *Scoble et al.*, 1997; *Kim and Moon*,  
 193 2013; *Konkan Railway Corporation*, 2012). This approach allows to elaborate directly the topographic  
 194 mapping data, which is more intuitive than the overbreak area approach. The admitted overbreak distance  
 195 depends on the position of the section in the blasting round. In fact, the drilling look out angle makes the  
 196 excavated contour bigger at the end of the round than at the beginning. The admissible overbreak distance  
 197 can be evaluated as a mean of the distance at round beginning and at round end (*Olsson*, 2010 - Figure 5).

198



199

200 **Figure 5. Scheme of plan view. Excavated contour compared with design contour all along one round (modified from:**  
 201 *Olsson*, 2010). The start cross section is smaller than the end one due to drilling lookout that is necessary to have enough  
 202 operative space.

203 The maximum overbreak distance ( $O_v$ ) depends on each national legislation and special conditions can be  
 204 arranged between the parts in the contract (*Olsson*, 2010; *Konkan Railway Corporation*, 2012). Scandinavian  
 205 countries present similar values of the admissible overbreak distances. Table 2 shows a comparison of the  
 206 excavation classes used in Sweden (*Anlaggnings AMA*) and Finland (*InfraRyl*) (*Olsson*, 2010).

207 **Table 2 Excavation classes of tolerance in Sweden and Finland (from: *Olsson*, 2010).**

Excavation tolerance	Maximum admissible distance expressed as
----------------------	--

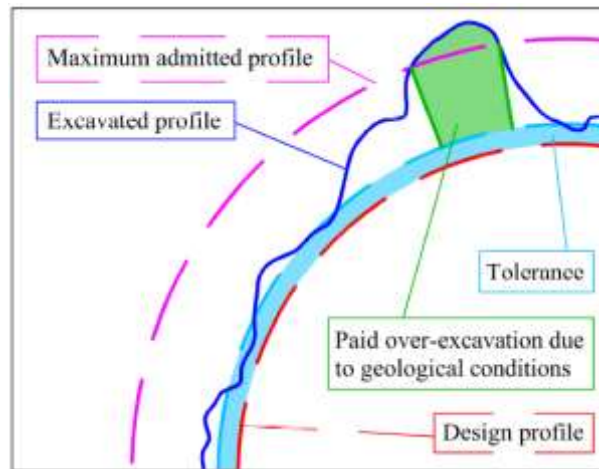
classes	average of round beginning and round end [m]		
	AMA - Sweden	InfraRyl - Finland	
		Walls and crown	Floor
1 - special class	0.30	< 0.20	< 0.20
2 - normal class	0.35	< 0.40	< 0.60
3 - tunnel access (first 10 m)	0.40	< 0.60	-
4 – special cases		No demands	No demands

208

209 Norwegian and Italian legislations come from the Swiss one (SN, 2004; NPRA, 2012). In these countries  
 210 the overbreak ( $O_v$ ) depends on the theoretical excavated area ( $A_d$ ) using Equation 3 as shown in Figure 66:

211 
$$O_v = 0.07 \times \sqrt{A_d} \tag{3}$$

212



213

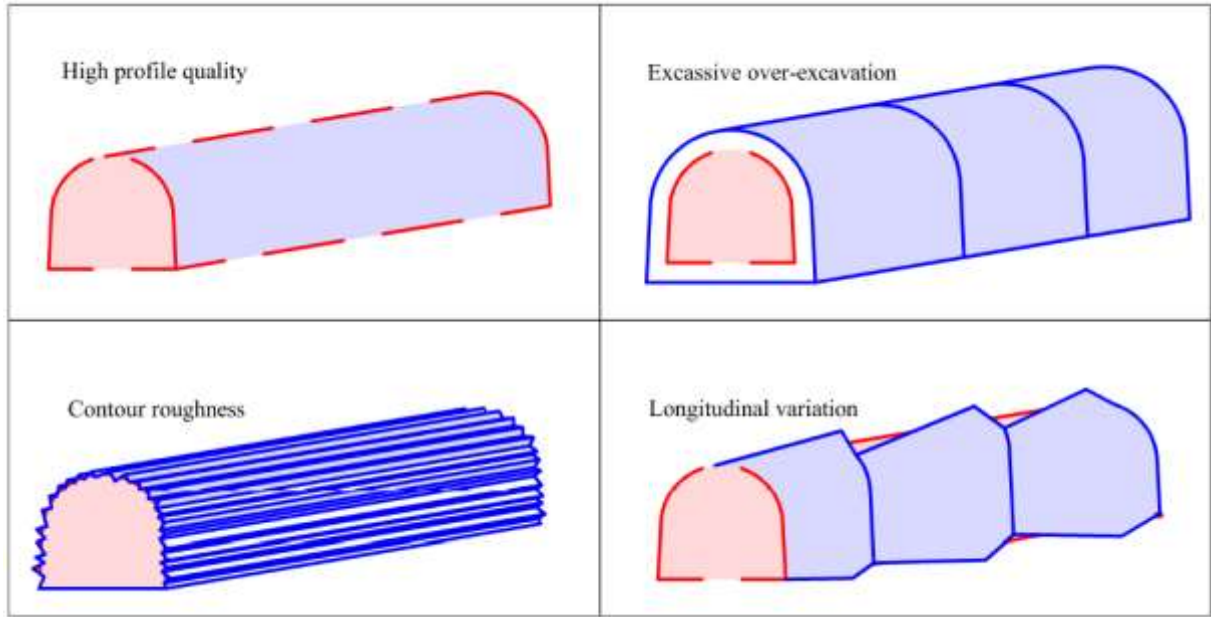
214 **Figure 6. Contractual profiles: the design profile presents a tolerance (light blue area) but the admissible over-excavation**  
 215 **is measured from the design profile (not from the tolerance) and depends on the minimum between Equation 3 and 0.4 m.**  
 216 **Outside the maximum admissible contour the over-excavation costs relapse on the contractor but the over-excavation costs**  
 217 **due to geological condition relapses on the client (green area) (modified from SN, 2004).**

218 All the evaluations on overbreak distance consider it outside the design contour because no rock within  
 219 the design profile is admissible (Mahtab et al., 1997; Olsson, 2010).

220 **3.3 Tunnel Contour Quality Index**

221 This index was developed (Kim, 2009; Kim and Bruland, 2010; Kim and Bruland, 2015) in order to  
 222 evaluate tunnel and rounds contour quality in D&B context. This index takes into account overbreak

223 distances of each cross-section ( $O_v$ ), contour roughness as ratio of contour length ( $RCL$ ) and longitudinal  
 224 overbreak variation ( $V_0$ ), as shown in Figure .



225  
 226 **Figure 7. Different effects of the parameters that affect the TCI (modified from: Kim, 2009). Excessive overbreak directly**  
 227 **affects muck volumes and final lining to reach the design contour; contour roughness influences lining and supports and can**  
 228 **cause under-excavation; longitudinal variation affects the operations of lining placement.**

229 Equation 4a relates these parameters for the entire tunnel where more than five consecutive rounds are  
 230 available, Equation 4b can be applied in each single round.

231 
$$TCI_{tunnel} = \frac{C_r}{W_1 C_1 \overline{O_v} + W_2 C_2 \overline{RCL} + W_3 C_3 V_0} \quad (4a)$$

232 
$$TCI_{round} = \frac{C_r}{W_1 C_1 O_{v\_round} + W_2 C_2 RCL_{round}} \quad (4b)$$

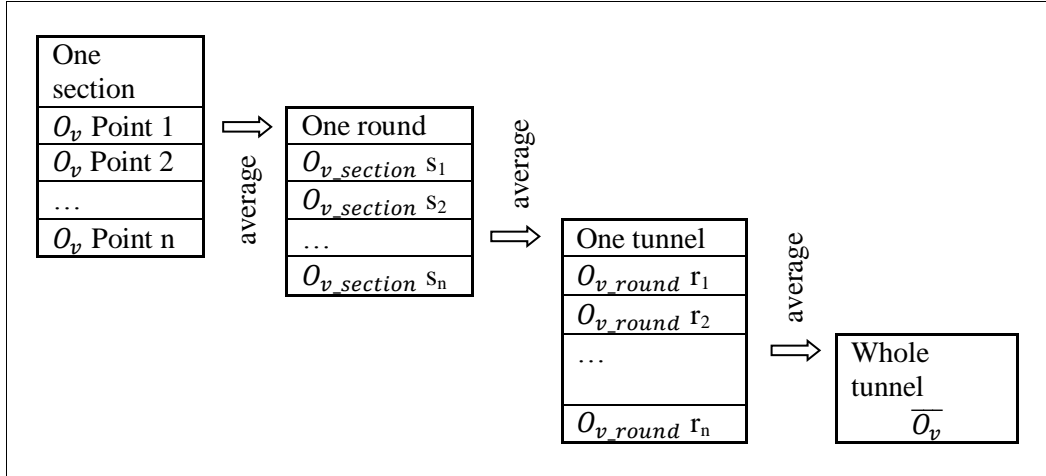
233 Where:

- 234 •  $C_r$ : constant of adjustment.  
 235 •  $W_1$ : importance of additional mucking.  
 236 •  $C_1$ : overbreak correction factor.  
 237 •  $\overline{O_v}$ : average of the rounds overbreak distance [cm].  
 238 •  $W_2$ : importance of additional shotcrete.  
 239 •  $C_2$ : contour length correction factor.  
 240 •  $\overline{RCL}$ : average of the round contour ratio.  
 241 •  $W_3$ : importance of longitudinal variation.  
 242 •  $C_3$ : longitudinal overbreak correction factor.  
 243 •  $V_0$ : longitudinal overbreak variation [cm], which is the round overbreak standard deviation.

244 The total overbreak is calculated with the following steps:

- 245 1.  $O_v$ : distances between excavated contour and design contour in many points of the same cross-
- 246 section.
- 247 2.  $O_{v\_section}$ : average value of overbreak distances (in cm) of each scanned section.
- 248 3.  $O_{v\_round}$ : average value of  $O_{v\_section}$  considering at least two sections in each round.
- 249 4.  $\overline{O_v}$ : average value of  $O_{v\_round}$  to consider the entire tunnel.

250 Figure 8 shows the practical way of the procedure.



251

252 **Figure 8. Scheme of the procedure that is necessary to calculate average overbreak, one of the main TCI parameters. The**  
 253 **procedure to obtain rounds and tunnel RCL is almost the same.**

254 Coefficients of adjustment have been calculated following the procedure well explained in *Kim (2009)*.

255 Equation 5 gives an example of their structure showing the overbreak coefficient equation.

256 
$$C_1 = \frac{1}{\left[ \left( \frac{1}{n} \sum_1^n O_{v\_round} \right) + 5 \times std(O_{v\_round}) \right]} \quad (5)$$

### 257 3.4 Profile survey

258 After rounds blasting, the geometry documentation is important both for owner and contractor, in order to  
 259 evaluate excavation quality, excavated volumes and supports (*Gikas, 2012*). Contact (finger probes, tape  
 260 extensometer and section profiler) and non-contact instruments (theodolite, total stations, photogrammetry,  
 261 optical triangulation and Terrestrial Laser Scanning – TLS) permit data acquisition (*Pejić, 2013*).

262 The methods that are mainly used are photogrammetric techniques, Terrestrial Laser Scanner (TLS) or  
 263 conventional survey with total station (*Olsson, 2010; Gikas, 2012*).

264 The photogrammetric techniques can give a 3D scan of the tunnel tube collecting each surface point at  
 265 least in two photographs. It is a quite low cost technique but is not common in underground works because  
 266 the surface is irregular and there is not enough light for taking quality pictures .

267 The Terrestrial Laser Scanner (TLS) can rapidly locate points with high accuracy (e.g. thirty meters can  
268 be scanned in ten minutes) and it provides a point cloud. The presence of reflective objects (e.g. equipment  
269 and water) can affect the recognition of targets (Gikas, 2012). Data can be shown in a virtual reality model  
270 and, if texture information are available, it is possible to render a photorealistic VR model (Chmelina, 2010).

271 The total station needs a calibration and some starting parameters are set manually: profiles interval,  
272 measuring angle, beginning and ending chainages; then total station could reveal points automatically with  
273 iterations. The instrument should be located as near as possible to the symmetry axis, in order to equilibrate  
274 the density of the points on the contour; this surveying method took about one hour each ten meters of  
275 tunnel. This procedure is usually done after scaling and shotcreting for safety reasons. Also the total station  
276 survey can be affected by the presence of reflective objects (e.g. equipment and water) as the TLS can be.

277 A profile-image method can also be used in tunnel works (Wang et al., 2009; Wang et al., 2010), joining  
278 laser profiling with photogrammetry to obtain a more accurate survey.

## 279 4. Methods

### 280 4.1 Data gathering

281 The study case is a roadway tunnel excavated in one of the North provinces of Norway. The tunnel is  
282 4585 m long with a face of about 80 m<sup>2</sup> of surface and lies under 300 m of overburden. The work was  
283 planned for a period of nine months (from August 2014 until April 2015). The tunnel was excavated by D&B  
284 using the Norwegian Tunnel Method of Tunnelling (NTNU, 1995) - NTM - that is the application of New  
285 Austrian Tunnelling Method - NATM- on hard rock. The construction was developed through competent  
286 metamorphic rock mass, composed by sandstones, slates and expansive clays with chlorites. The Q index,  
287 obtained from visual inspection of the tunnel face, was used as classification of the ground condition. The  
288 available data from geological site survey list 54 rounds located from kilometric point KP 5561.9 to 5781.8  
289 (47 surveys) for Portal 1 and from KP 10127.5 to 10107.5 (7 surveys) for Portal 2 of the tunnel. Three main  
290 joint set families were observed along the rounds excavated (as from the geotechnical report). Table 3  
291 describes the relative range of dip and dip direction of these main joint sets with respect the tunnel axis.

292 **Table 3. Basic data for the main joint sets.**

Orientation of the main joint sets observed	
Joint set (S)	Dip / Dip Direction (°)
S1	45 – 70 / 235 - 255
S2	60 – 80 / 010 - 020
S3	40 – 65 / 095 - 120

293

294 Two jumbos Atlas Copco XE3C and XE3D of three booms each, equipped with percussive-rotary top  
295 hammer drilling mechanism, working in semi-automatic ABC total system were used to drill the analysed

296 blast rounds. Available data concern production face drilling holes of short length (4.0 – 5.5 m), drilled by  
297 using only one rod (5.5 m length and 38 mm diameter) and a bit of 46 mm diameter.

298 The charging of the blastholes was carried out with emulsion of different lineal charge according to the  
299 type of blasthole; nominal charging information estimate theoretical lineal charges of 1.6 kg/m, 1.2 kg/m,  
300 0.85 kg/m and 0.5 kg/m for cut/lifter, stopping, second contour and contour holes, respectively. The nominal  
301 number of blastholes per round was about 140; this counted about 16 cut holes, 12 lifter holes, 57 stopping  
302 holes, 24 second contour holes and 32 contour holes. Stemming was estimated in 0.4 m for all blastholes  
303 with exception of contour holes that were not stemmed. The firing was bottom initiated with booster and  
304 non-electric detonators; nominal timing reports indicate the use of LP non-electric detonators from numbers  
305 0 to 60. Round progress was 93% of the drilled length and production was estimated at 1.6 blasts per day;  
306 this is a progress of about 7.2 meter per day. The excavation was made simultaneously from the two sides of  
307 the tunnel.

308 Portal 1 and 2 were located at 105 m a.s.l. and 6.75 m a.s.l. respectively. Starting from Portal 1, the tunnel  
309 was upwards oriented with a slope of 1.5% for about 617 m, followed by a downhill of a -2.5 % slope until  
310 Portal 2. Tunnel cross section dimensions were decided considering the estimation of traffic volume twenty  
311 years after the opening (Annual Average Daily Traffic volume – AADT) and the tunnel length (NPR, 2004);  
312 AADT was estimated between 7500 and 9500 units. In order to fulfil this traffic volume, most of the  
313 cross-sections follow the Norwegian type section T9.5 (theoretical excavated area 74 m<sup>2</sup>) apart a widening  
314 zone of the tunnel that follows the cross-section T12.5 zone (theoretical excavation area 100 m<sup>2</sup>), for a length  
315 of about 30 meters. The face area of the two transition zones, before and after the widening, 30 m long each,  
316 was increased (or decreased) regularly until matching the respective cross-section, namely that of T9.5 and  
317 T12.5.

318 Table 4 shows the measurements for the used cross sections, referred to Figure 9. The design area starts to  
319 increase from chainage (KP) 5785 until KP 5815 to reach the T12.5 section between KP 5815 and KP 5845.  
320 Then it decreases until KP 5875.

321 Topographical mapping of the excavated void after blasting was surveyed with a total station Leica Viva  
322 on the shotcreted surface; set angle was chosen to reveal approximately one point each 50 cm on the contour.  
323 Typical thickness of the shotcrete liner lies between 80 and 100 mm.

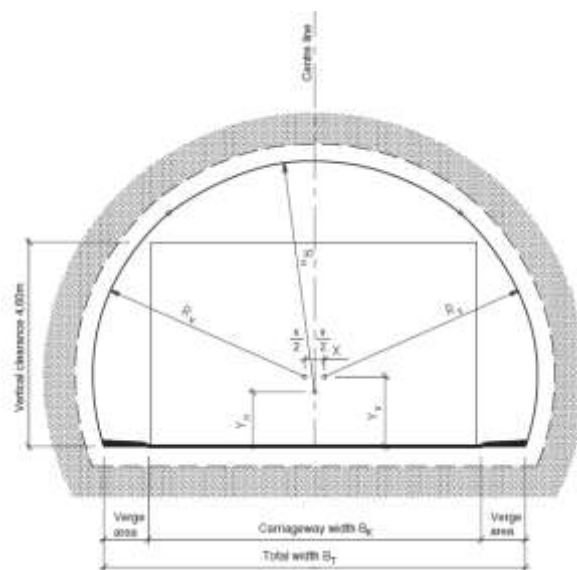
324 Cross-section profiles perpendicular to the direction of the tunnel axis of the excavated face were  
325 extracted at every 1 m in AutoCAD files. Each profile was identified by its respective kilometric point; this  
326 comprises a total of about 500 excavated profiles measured.

327 **Table 4. Geometric measurements for tunnel cross-section that was used in this case study (from: NPR, 2004; Tunnel**  
328 **project documents).**

Geometric measurement	Section T9.5	Section T12.5
-----------------------	--------------	---------------

Total width ( $B_T$ )	9.50 m	12.50 m
Carriage way width ( $B_K$ )	7.00 m	10.00 m
Lanes	$2 \times 3.50$ m	$3 \times 3.50$ m
Shoulder (in verge area)	$2 \times 1.00$ m	$2 \times 1.00$ m
Sidewalk (in verge area)	$2 \times 0.25$ m	$2 \times 0.25$ m
Centre point wall radius ( $X$ )	0.44 m	3.44 m
Centre height wall radius ( $Y_V$ )	1.57 m	1.57 m
Wall radius ( $R_V$ )	4.79 m	4.79 m
Centre height lining radius ( $Y_H$ )	1.22 m	-0.46 m
Lining radius ( $R_H$ )	5.20 m	7.45 m
Vertical clearance	4.60 m	4.60 m
Nominal area	66.53 m <sup>2</sup>	91.23 m <sup>2</sup>
Concrete upholstery	0.60 m	0.60 m
Excavation area	74m <sup>2</sup>	100m <sup>2</sup>

329



330

331 **Figure 9. Geometry of tunnel cross-section T9.5 and T12.5 (NPR, 2004).**

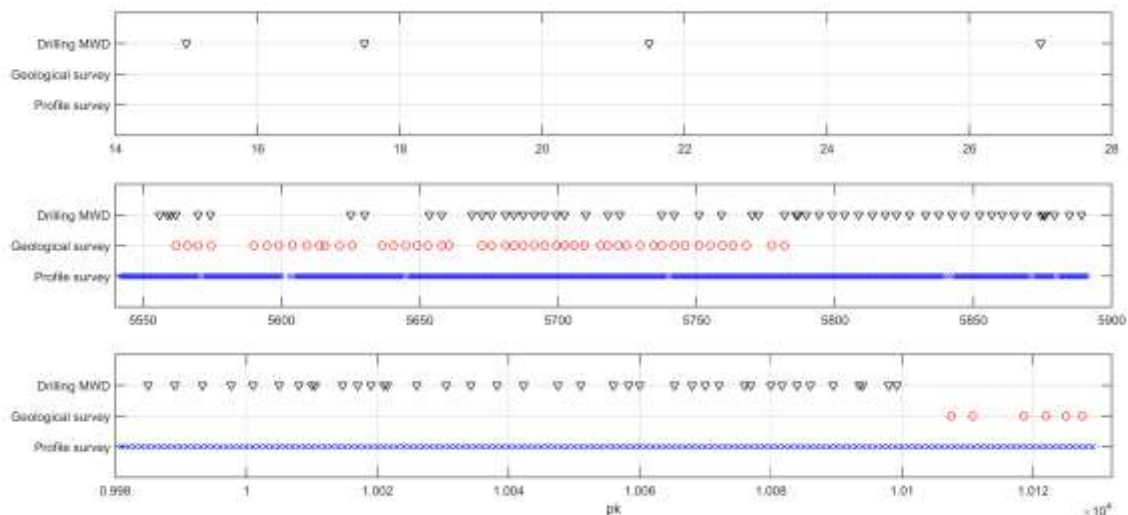
332 **4.2 Data analysis**

333 The aim of the survey is to assess the quality of the resulting contour from the excavated profiles  
334 compared with the theoretical section intended. Since the actual lineal charge of the holes is not available,  
335 the explosive is considered as a constant variable. Therefore, differences in the excavation sections (over-  
336 excavation and under-excavation) should be mainly generated by a variation in the geotechnical rock  
337 characteristics. The work developed by *Costamagna* (2016) is applied here in order to evaluate round blast

338 results in terms of overbreak and TCI. For this reason, a Matlab script has been developed in order to  
339 automatically make uniform and treat three kinds of data (Figure 10):

- 340 1) Scanned profiles (about 500 *.dxf* files)
- 341 2) Geotechnical characterization (54 surveys)
- 342 3) Drilling data (measurements while drilling, about 11700 *.MWD* files)

343



344

345 **Figure 10. Analysed data as function of the chainage. The blue crosses show the scanned cross-sections, red circles show**  
346 **the beginning KP of the geological surveys and black triangles show the nominal position of start drilling sections where**  
347 **MWD data are collected.**

348 The data collected by means of the geostructural survey allowed to set the Q-system parameters. The other  
349 rock mass damage indices (i.e. BDF, BDI, FAI) could not be evaluated in this case study.

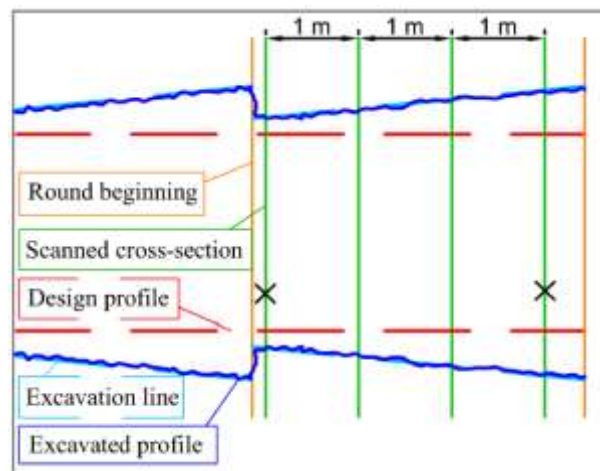
350 In order to evaluate round results and compute some of the parameters used to assess TCI, it is necessary  
351 to identify each round and the cross-sections that belong to each of them. The KP of a new round is  
352 measured topographically. In the case study, the KP was measured both manually, by using a total station  
353 (used to reference the geotechnical reports), and automatically through the MWD system. The drilling jumbo  
354 has a laser scanner installed in its front side. During the positioning of the jumbo and before the drilling of a  
355 new round starts, the jumbo is aligned with the tunnel axis, by making pass through two targets located in  
356 one of the boom a laser beam aimed in the direction of the tunnel axis. The laser scanner also measures the  
357 distance to the face of the new round and records the kilometric point (here intended as the nominal KP) at  
358 which it is located inside the tunnel.

359 When MWD has been correctly measured and recorded, the mode of all  $z$  coordinates (borehole position  
360 along the longitudinal axis referenced to the nominal KP) in each drilled section is added to their nominal  
361 KP, in order to consider also the irregular face surfaces.



362 In case no MWD data is available for adjacent rounds, the KP taken from the geotechnical reports is used.  
 363 KPs from the MWD system in which  $z$  coordinates records have failed for all boreholes and taken from the  
 364 geotechnical reports may induce some error in the beginning of the round (due to irregularities in the face)  
 365 and also occasional overlapping between two adjacent rounds (as for the 93 % round progress). Since cross-  
 366 sections are scanned at every 1 m depth, a correction for clustering excavated areas between two adjacent  
 367 rounds has been carried out by adding a length of 0.5 m to the initial KP, in order to reduce these KP errors.  
 368 In addition, rounds shorter than three meters have been rejected because at least three cross-sections in each  
 369 round are necessary for the round analysis and the maximum length per round has been identified by using a  
 370 robust variance estimator (*Miller and Miller, 2010*) and considering site work conditions. Therefore, rounds  
 371 between 3 to 5.5 m lengths have been considered for the analysis; this comprises 84 available rounds.  
 372 Scanned cross-sections within the kilometeric points of two adjacent rounds of the MWD system will be  
 373 framed in their respective round. Finally, the first and the last profile of each round have been discarded  
 374 because their blasting results can be affected by the above errors commented (Figure 11).

375



376

377 **Figure 11. Round plan view. Each scanned profile (green line) is assigned to its round, using beginning and ending round**  
 378 **KP. First and last profiles (orange lines) of each round were discarded because their blasting results can be affected by**  
 379 **drilling operations or blast results.**

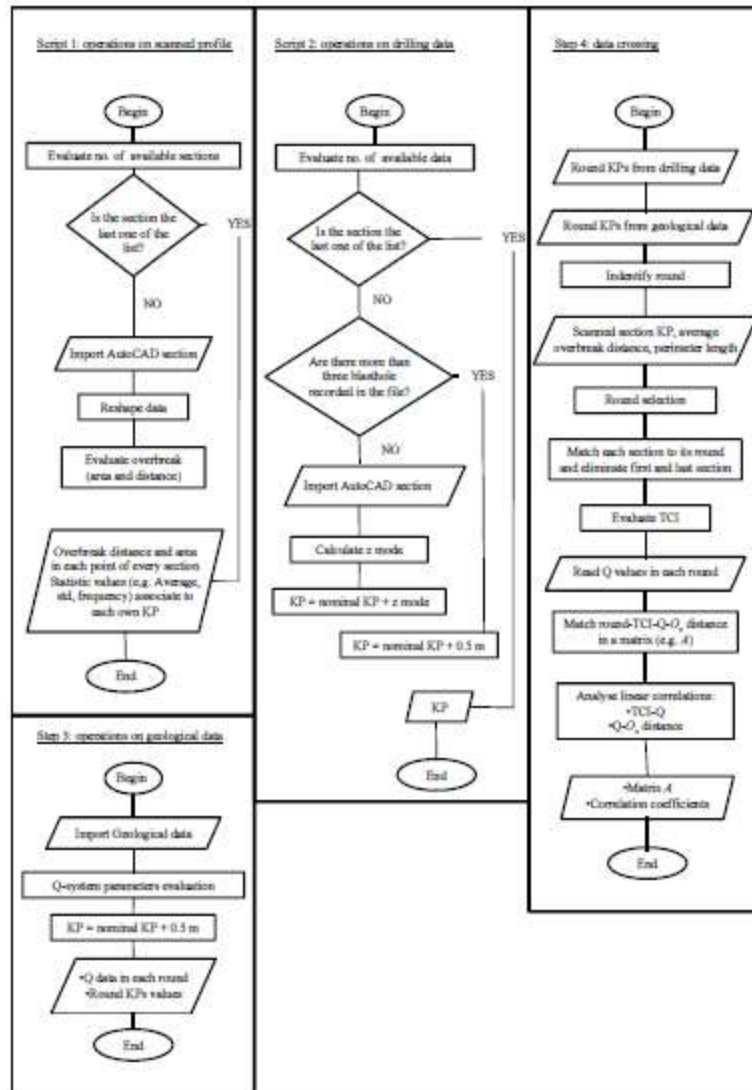
380 The overbreak has been evaluated based on distances and areas. The overbreak is defined in two ways:

- 381 • Over-excavation: it is the extra void outside the design contour line. It is evaluated as positive  
382 overbreak.
- 383 • Under-excavation: it is the void inside the design contour line. It is evaluated as negative  
384 overbreak.

385 This distinction is necessary for the correct evaluation of the overbreak. In fact, the over-excavation  
 386 affects the shotcrete thickness, the rock support and the mucking; the under-excavation is not admitted in the  
 387 contracts and it affects the scaling.

388  
389

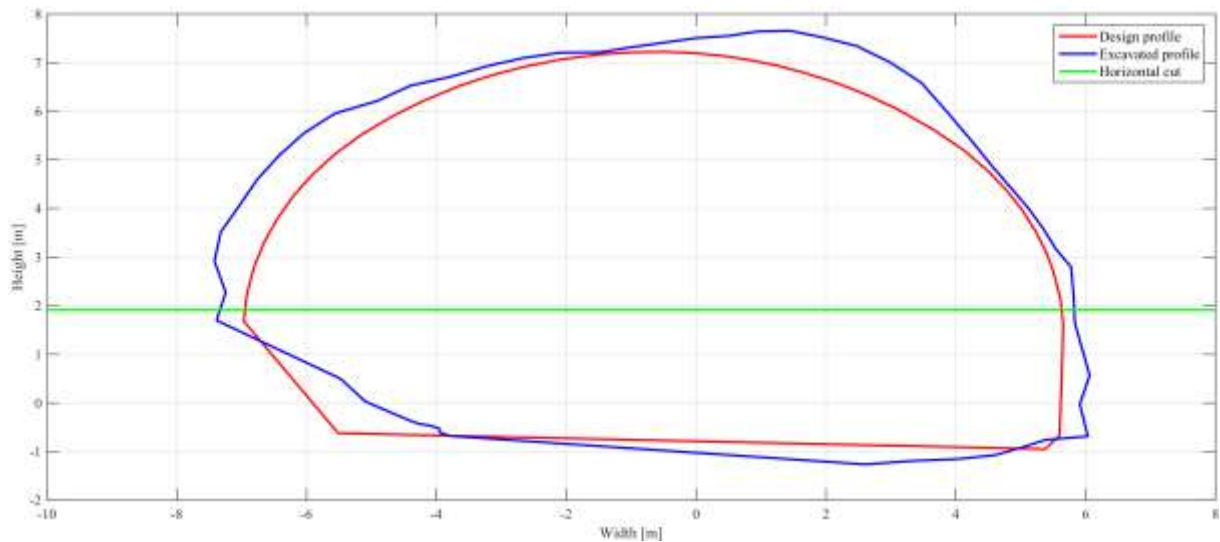
Figure 12 resumes in four steps the data treatment and matching.



390

391 **Figure 12. Flow chart of the first three step of the analysis. Step 1 elaborates data from profile survey, working from .dxf**  
392 **files and return a structure that contain, among others, statistical evaluations on overbreak (that are used after). Step 2**  
393 **works on geological data (from .xls file) and evaluates Q system factors. Step 3 calibrates round beginning-end kilometric**  
394 **point proceeding from drilling data (.MWD). Step 4 matches each scanned profile to its own round and calculate TCI. It also**  
395 **evaluates the correlation TCI - Q value and over-excavation - Q in each round.**

396 In this paper, cross-section contour have been analysed on the 65% upper part as shown in Figure 13.  
397 This choice depends on the low quality of the floor and corner profile survey: these bad data corrupt the  
398 results showing an unrealistic under-excavation, but the horizontal cut erases their contribution in almost  
399 every section.



400

401

402 **Figure 13. Section KP = 5799. The horizontal line is set at 35% of tunnel height to keep out the corner of the cross-**  
 403 **section. All the data about over-excavation that are used for the results and discussion comes from the contour above the**  
 404 **horizontal cut. In this way the most of profile scanning errors are not considered.**

405

## 5. Results and discussion

406

407

408

409

410

411

412

413

The automatic analysis mentioned in the previous section collects, selects and treats a huge number of data. This section presents the results validated in a case history focusing on the overbreak (both in area and distance evaluation), trying to correlate them with the Q-system classification. Based on available data and on Equations 4a and 4b, TCI values are consequently processed. This index could allow time and costs reduction because it mainly uses profile scanning data that can be collected and analysed automatically. Anyway, to make its use easy and efficient, an extensive casuistry is required to build a TCI-value classification. Data reported in this study can improve the database and the evaluations required to build a related classification.

414

415

416

417

As said, all the evaluations on cross-section contour have been done on the 65% upper part (hereafter no more specified), in order to avoid survey inaccuracy. In fact, the survey was probably affected by the presence of muck left in place, disturbance due to ventilation system or water particles that reflected the laser ray in a wrong way (Gikas, 2012).

418

### 5.1 Tunnel quality indicator: overbreak

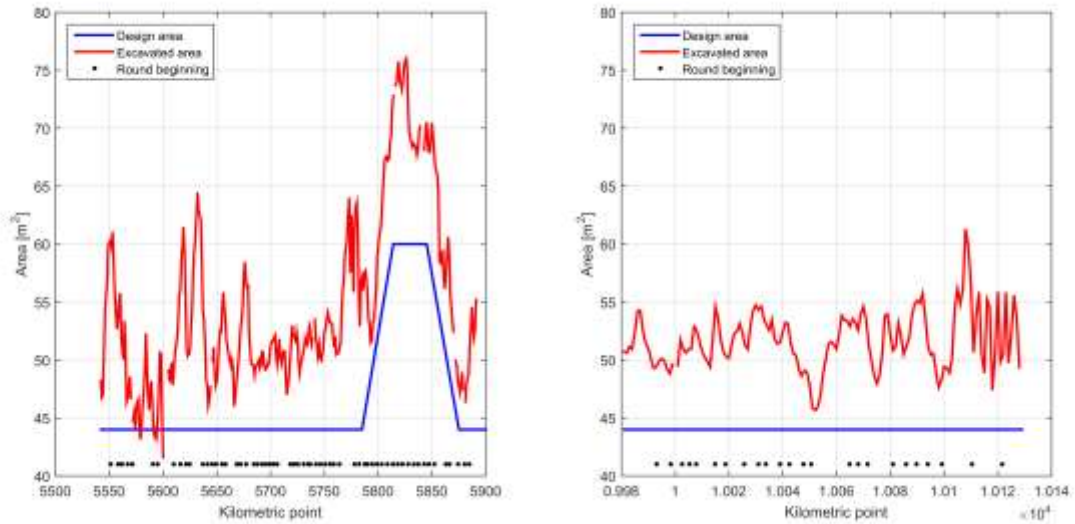
419

420

421

422

The beginning of the round corresponds to minimum peaks of the excavated area. In fact the end of each round must be larger than round beginning due to the drilling lookout. This trend is confirmed as shown in Figure 14.

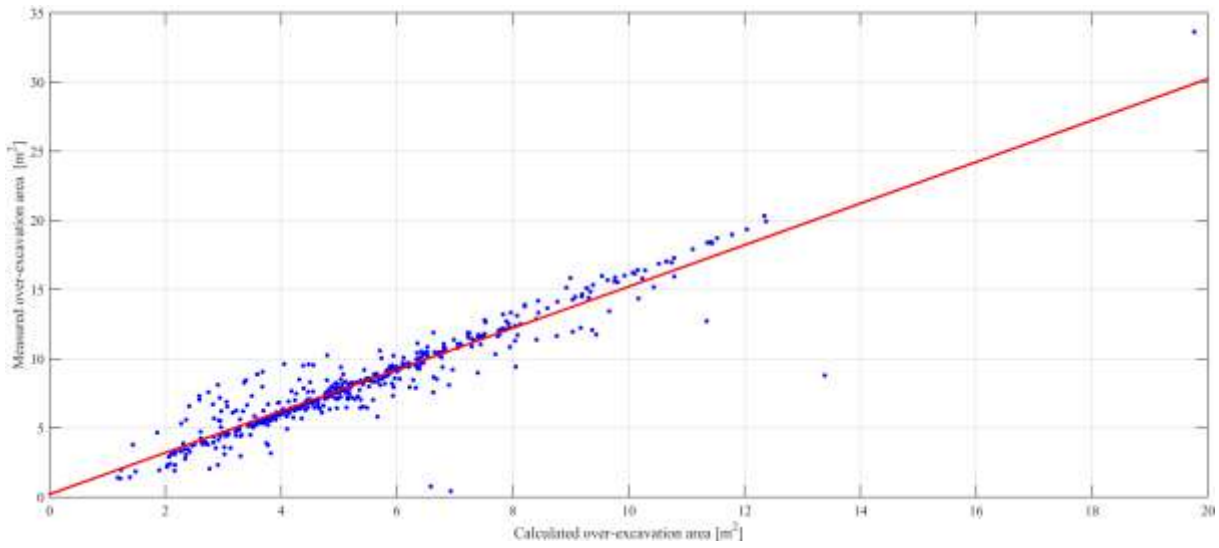


423

424 **Figure 14. (left) Areas of the 65% upper zone of the cross section surveyed from Portal 1. (right) Areas of the 65% upper**  
 425 **zone of the cross section surveyed from Portal 2. Blue line shows the design area above the horizontal cut and interpolates the**  
 426 **theoretical values in the increasing/decreasing segments. Black points show the beginning KP of the analysed rounds.**

427 Most of the cross-sections do not present under-excavation, as it should be. Anyway some exceptions,  
 428 especially section from KP 5570 to KP 5603 and from KP 10004 to KP 10013 present under-excavation due  
 429 to errors during the contour scanning. However, the actual area is still bigger than the design one because the  
 430 over-excavation compensates the under-excavation area. Anyway, the following results concern the over-  
 431 excavation and omit any deeper consideration on under-excavation because, as said, it is not admissible and  
 432 affects scaling costs.

433 The over-excavation is measured as distance during the surveys but the over-excavation additional costs  
 434 depend on volume of additional muck and voids that needs to be shotcreted. These volumes can be  
 435 calculated a posteriori from the over-excavation area of each cross-section. In this case study, the developed  
 436 code measures over-excavation area (that correspond to a volume for unit of advance - 1 m) from polygons  
 437 between design and actual contour but it can be correlated to the average over-excavation distance and the  
 438 design contour length, as shown in Figure 15. The two values are linearly correlated: 1.50 slope in a range of  
 439 [1.45; 1.55], 0.20 intercept in a range of [-0.09; 0.50], 0.88 of  $R^2$  value.



441

442 **Figure 15. Over-excavation area can be calculated as function of average overbreak distance ( $\bar{O}_v$ ) and design contour**  
 443 **length ( $D_l$ ), using the relation  $O_{v, \text{calculated area}} = \bar{O}_v \times D_l$ . This relation allows to consider only distance values.**

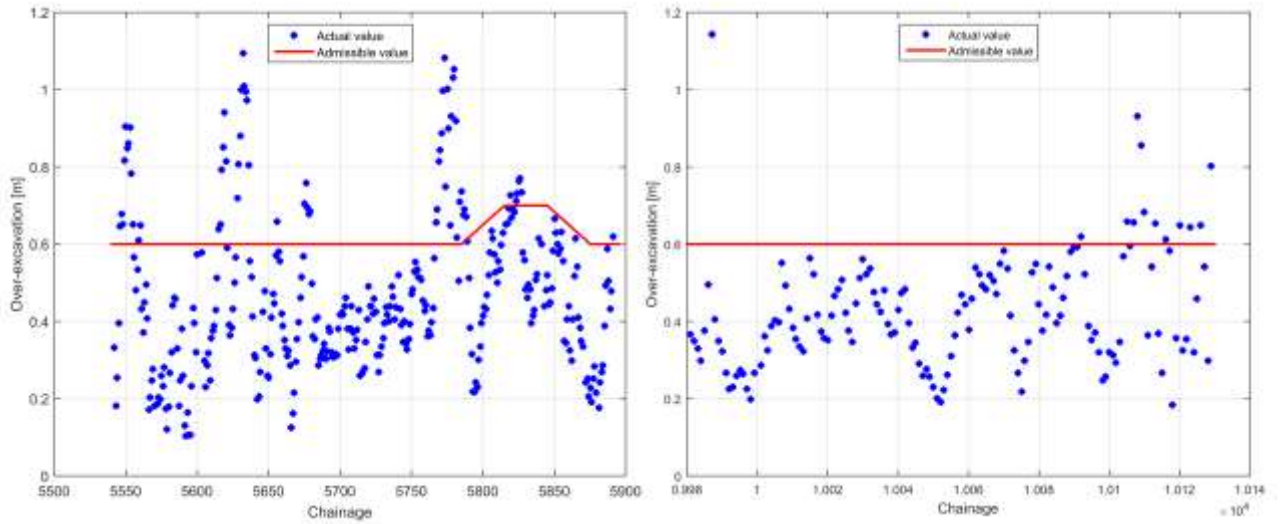
444 This relation allows to work only on over-excavation distance, as most of the literature does. However, in  
 445 some cases (*Mahtab, 1997; Mandal and Singh, 2009; Olsson, 2010*) the over-excavation normalized area (as  
 446 shown in Equation 2) is used. In this case study the average value of the over-excavated ratio is quite similar  
 447 for the sections from Portal 1 (18.5%) and from Portal 2 (17.1%). Considering all section from both portals,  
 448 the value is  $18.1 \pm 7.7\%$  (mean and standard deviation), in a range between 1% and 46%. Values from  
 449 literature are in a range between 7.3% up to 51.9% (*Mahtab, 1997; Mandal and Singh, 2009; Olsson, 2010*)  
 450 and *Olsson (2010)* proposes an admissible overbreak ratio of 25% as upper limit.

451 According to the Norwegian regulation the admissible over-excavation ( $O_v$ ) is the minimum value  
 452 between 0.4 m and the value calculated as function of cross-section area (Equation 3, Table 5). A third limit  
 453 is interpolated and used to evaluate all the cross-section in which the area progressively increases/decreases  
 454 due to switch between theoretical section T9.5 and T12.5. No references for these sections were found in  
 455 literature.

456 **Table 5. Maximum admitted  $O_v$  depending on cross-section area and evaluation of case study available sections.**

Theoretical cross-section	Area [m <sup>2</sup> ]	Maximum admissible $O_v$ [m]	No. of sections	Compliant sections (% on their group)
T9.5	74	0.60	400	84
T12.5	100	0.70	28	79
Interpolation	[74; 100]	0.65	59	92

457



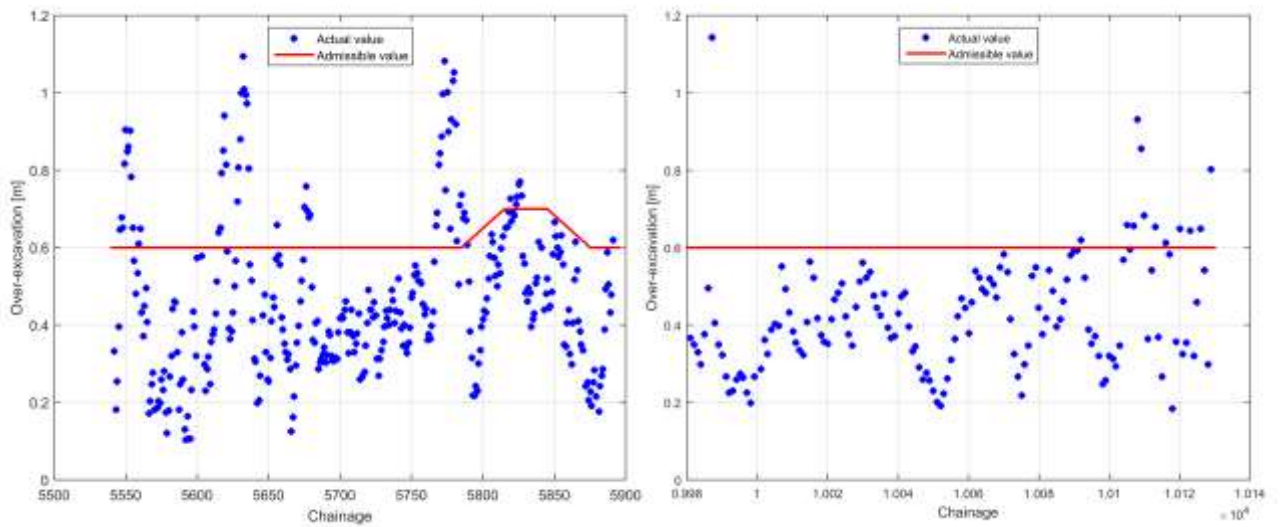
458

459 Figure shows the average value of the over-excavation distance for each scanned section and the  
 460 threshold values. Average values of over-excavation of each cross-section from both Portals are considered  
 461 to obtain average, maximum and minimum values for the entire tunnel (Table 6).

462 **Table 6. Evaluation on overbreak distances.**

Values on sections from Portal 1 and Portal 2		$O_v$
Average [m]		0.46
Standard deviation [m]		0.19
Maximum [m]		1.10
Minimum [m]		0.10

463



464

465 **Figure 16. (left) Average over-excavation distance in each section from Portal 1 compared with admissible values. (right)**  
 466 **Average over-excavation distance in each section from Portal 2 compared with admissible values.**

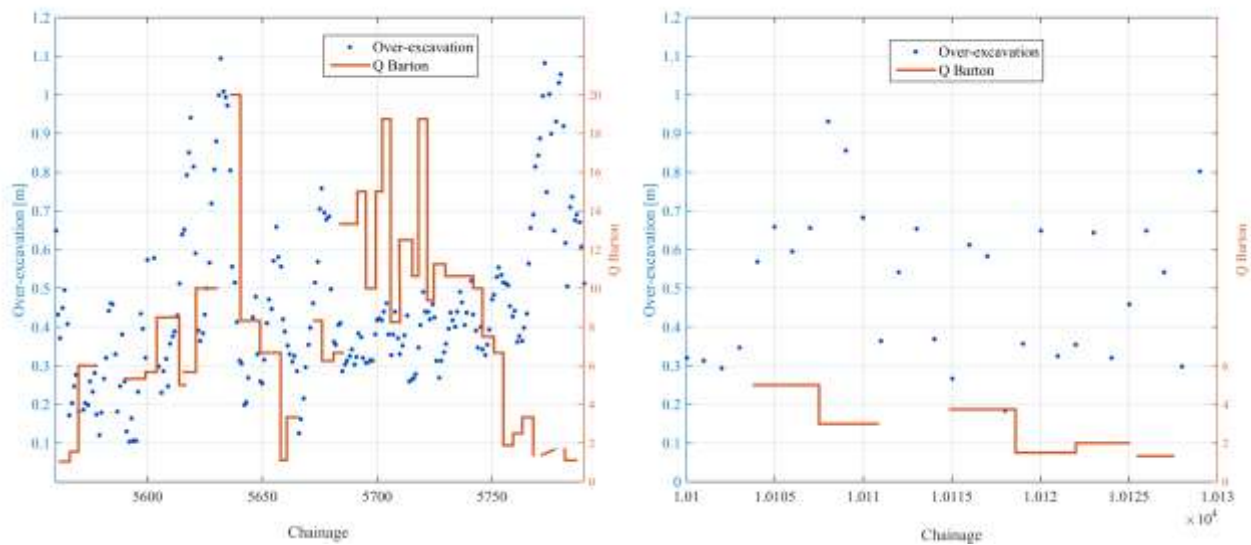
467 **5.2 Correlation between geological and topographical survey**

468 The main values for all the Q-system parameters suggest a fair-good rock (*RQD*) with an irregular and  
 469 smooth undulating surface ( $J_r$ ), usually two or three joint sets were surveyed plus some random joint ( $J_n$ ) and  
 470 the most of these joint were slightly altered ( $J_a$ ); the rock mass is medium stressed (*SFR*). The surveyed rock  
 471 mass is dry, and the value  $J_w$  is constantly set on 1. As summary, the rock mass can be considered very poor -  
 472 poor - fair (classes IV, V, VI) quality all along the tunnel.

473 Under the assumption that every drill an blast cycle was done with the same technique and the same  
 474 equipment, available geology data are compared with overbreak distances.

475 Figure 17 shows Q progression along the tunnel axis and overlaps average over-excavation of each  
 476 scanned profile.

477



478

479 **Figure 17. (left) Over-excavation distance and Q of each scanned or surveyed section from Portal 1. (right) Over-**  
 480 **excavation distance and Q of each scanned or surveyed section from Portal 2.**

481 Average over-excavation of each round is compared with the Q value trying to demonstrate a relation  
 482 between Q index and excavation results. 18 rounds present enough data to be analysed in this case; no linear  
 483 correlation was found between the average over-excavation distance and Q values. Table 7 shows the range  
 484 of over-excavation distances for each Q classes. These ranges are similar for all the classes and they cannot  
 485 be used to predict the blasting results in each round.

486 This lack of correlation could depend on shotcreting phase, as it modifies in sense of smoothing the  
 487 contour profile. In fact, best rock mass quality should require less shotcrete (and the opposite on low quality

488 surfaces), thus over-excavation results are emphasised (or mitigated). But available data do not allow  
 489 confirming this hypothesis, thus shotcreting thickness has been considered as a relatively constant value.

490 **Table 7. Over-excavation ranges in Q classes.**

	Over-excavation [m]			
	Min	Max	Mean	Std
$Q \leq 4$	0.35	1.50	0.75	0.36
$4 < Q \leq 10$	0.16	1.23	0.64	0.26
$10 < Q \leq 40$	0.42	0.94	0.64	0.20

491

### 492 **5.3 Tunnel quality indicator: Tunnel Contour Quality Index (TCI)**

493 The Tunnel Contour Quality Index - TCI (3.3) can be evaluated for each round.

494 Equation 4b has been used, following the procedure well explained in *Kim* (2009) for the coefficient  
 495 determination. Table 8 shows the values used in this case study to calculate TCI in each round and for the  
 496 whole tunnel.

497 **Table 8. Values of TCI coefficients and weight.**

Coefficient of adjustment		Weight <sup>a</sup>	
$C_1$	0.0049	$W_1$	4.5
$C_2$	0.6765	$W_2$	4.5
$C_3$	0.0206	$W_3$	1.0
$C_r^a$	300		

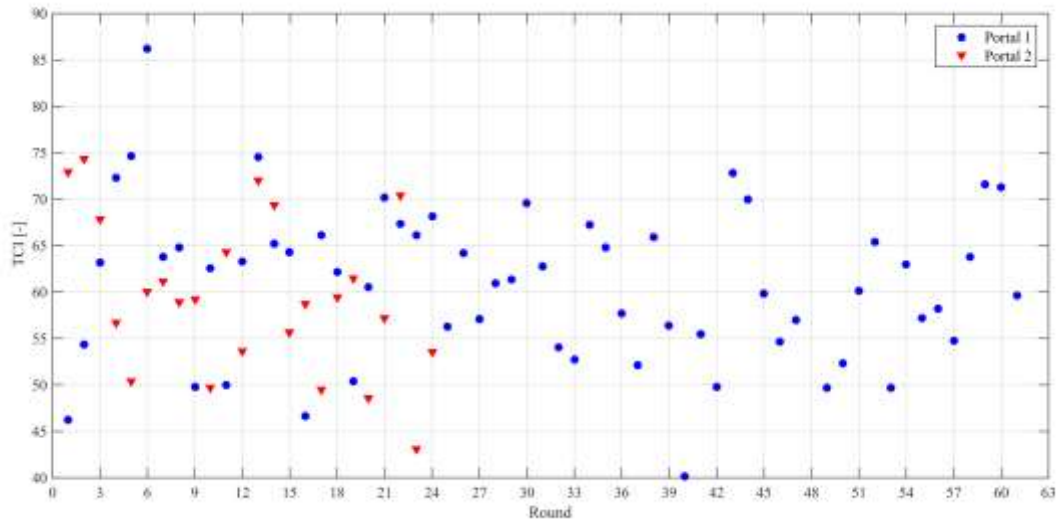
498 a) values obtained by *Kim* (2009)

499 b) values calculated by using this case data and following Equation 5

500

501 TCI obtained values vary from 40 up to 86; the two Portals do not present different ranges of this value,  
 502 and they can be analysed together (Figure ).



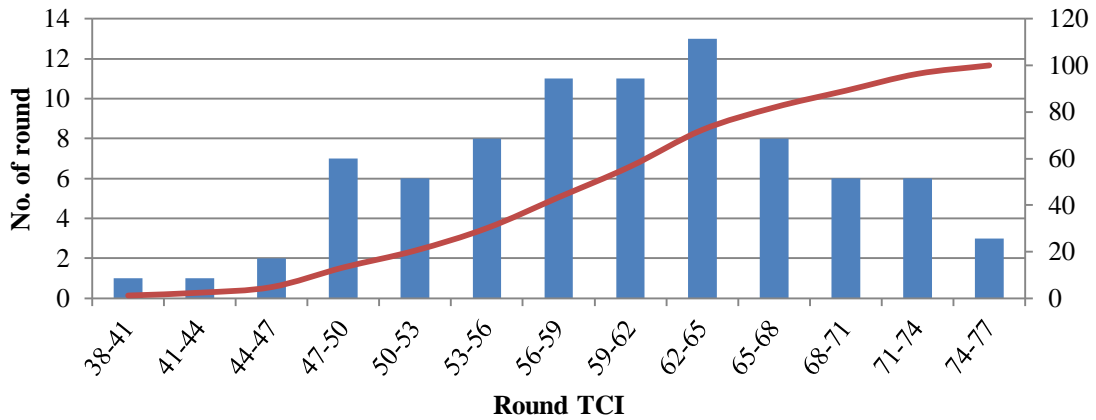


504

505 **Figure 18. TCI in each round from Portal 1 and Portal 2. The most of the values are between 45 and 75 in both Portals.**

506 The distribution of round TCI is shown in Figure 9 according to the classes that were proposed in  
 507 literature (Kim, 2009). The largest frequency is found between 62 and 65; the whole range is between 38 and  
 508 77. The case study presents good round TCI compared with literature case studies (Table 9).

509



510

511 **Figure 19. Distribution and cumulative distribution of round TCI based on case study data.**

512 **Table 9. Comparison with round TCI results from literature (Kim, 2009; Kim and Bruland, 2010) and case study tunnel.**

Tunnel	Minimum round TCI	Maximum round TCI	Largest frequency
LS02 (Norway)	38	62	47-50
Marienberg (Norway)	47	58	53-56

Misiryung (Korea)	56	75	62-71
Case study	38	77	62-65

513

514 TCI can be evaluated on the whole tunnel if more than five rounds are available (*Kim, 2009*). Table 10  
515 shows the values of the index parameters in the case study, comparing the resultant TCI with literature  
516 examples (*Kim, 2009; Kim and Bruland, 2010; Kim and Bruland, 2015*). The TCI value shows a good tunnel  
517 contour quality, quite near to the result in Misiryung tunnel that was considered to have a very good  
518 excavation result.

519 **Table 10. Comparison of TCI in different studies.**

TCI parameter	Case study
$C_1$	0.0049
$C_2$	0.6765
$C_3$	0.0206
Average $O_v$ [cm]	70.2
Average RCL	1.2
$V_0$	5.4
<b>TCI</b>	<b>57.4</b>
Tunnel TCI from literature	
LS02 (four segments)	48.2
Marienburg	52.1
Misiryung	62.4

520

## 521 **6. Conclusions**

522 In this paper, tunnel contour evaluation is obtained in terms of overbreak and related to rock mass  
523 conditions. Over-excavation affects timing and costs (i.e. mucking and concrete/shotcrete costs), because the  
524 additional excavated volume usually needs to be replaced by additional shotcreting and other reinforcing  
525 works. In order to achieve a reliable procedure, the quality of almost 500 m of a roadway tunnel has been  
526 evaluated. For this purpose, measurements from three different sources are automatically processed:  
527 topographical measurements of excavated contour, geological mapping of the rounds and Measuring While  
528 Drilling (MWD) data.

529 According to the discussion, the work is related with the analysis of resulting profiles from D&B  
530 tunnelling and has provided the following main results:

- 531 1. A detailed analysis of large data sets is only possible by processing automatically the data. A code  
532 developed in Matlab environment has been created to quantify the overbreak caused by blast; it  
533 processes automatically MWD, geological and topographic data and stores them in the same  
534 numerical format. This code can be easily adapted to other case studies.
- 535 2. Results from the analysis are mainly focused on the characteristics of the excavated contour in  
536 comparison with the theoretical section, considering over-excavation in terms of area and distance  
537 separately and demonstrates that they are close linearly correlated. The study case exhibits an over-  
538 excavated distance of  $0.46 \pm 0.19$  m (mean and standard deviation). This value is in general under the  
539 admissible Norwegian limit of 0.6 up to 0.7 m calculated on the theoretical area.
- 540 3. The quality of data in the study case allows to focus only on geological causes and Q index is  
541 adopted to describe rock mass conditions. Q index exhibit from a very poor to fair quality. No strong  
542 numerical correlation between Q and over-excavation has been found. This result probably suggests  
543 that drill operations and blast design influence are stronger on contour quality control.
- 544 4. Tunnel quality has been also evaluated using the engineering index TCI. In the case study TCI has a  
545 value of  $60.5 \pm 8.4$ ; the largest frequency is found between 62 and 65; the whole range between 38  
546 and 77. These values are relatively well with those for other tunnels in literature. As more than five  
547 rounds are available, the index can be evaluated for the entire tunnel: overall TCI value is 57.4 and  
548 shows a quite good quality of the excavation (if compared with the studies of the index developer).

549 Further works based on the application of TCI to other case studies could enlarge the records and validate  
550 the efficiency of the index itself. The impact of shotcrete thickness should be deeply evaluated when the  
551 survey is done after shotcreting (as in this case) and more parameters should be recorded during the blast  
552 (e.g. PPV) in order to calculate other damage indices (e.g. BDI) and find out the most representative in terms  
553 of correlation with over-excavation. In the field of engineering application, the TCI index can provide a tool  
554 to evaluate tunnel contour quality in a unique way, simplifying the contractual requirements.

555

## 556 7. Acknowledgements

557 This work has been conducted under the project "VOLADAPT" (RTC-2014-2237-5) funded by the  
558 Spanish Ministry of Economy, Industry and Competitiveness under the program RETOS - Colaboración  
559 2014. The authors would like to thank to OSSA Obras Subterráneas SA, for providing the necessary data.

560

## 561 8. References

562 Barton, N., Lien, R., Lunde, J., 1974. *Engineering Classification of Rock Masses for the Design of Tunnel*  
563 *Support*. Rock Mechanics, vol. 6, n. 4.

564 Barton, N., 2007. *Rock quality, seismic velocity, attenuation and anisotropy*. Taylor & Francis Group,  
565 London, UK.

566 Barton, N., Grimstad, E., Palmstrom, A., 1995. *Design of Tunnel Support*, in: *Sprayed concrete: Properties, Design and Application*(Austin S.A. and Robins P.J.). Whittles Publishing, pp. 150-170.

567

568 Cardu, M., Mancini, R., Oggeri, C., 2004. *Ground Vibration Problems in the Excavation of Tunnels under Small Rock Cover*. In: Özgenoğlu, A., Yesilay, A.Y. (Eds.), *Environmental Issues and Waste Management in Energy and Mineral Production*, Kozan Ofset, Ankara.

569

570

571 Chmelina, K., 2010. *A virtual reality visualisation system for underground construction*. In: Beer, G. (Ed.), *Technology Innovation in Underground Construction*, CRC Press, London, UK.

572

573 Costamagna, E., 2016. *Quality control of D&B tunnelling profile with scanning systems*. MSc graduation  
574 thesis. Politecnico di Torino. Unpublished.

575 Gikas, V., 2012. *Three - Dimensional Laser Scanning for Geometry Documentation and Construction Management of Highway Tunnels during Excavation*. *Sensors*, 12(8), 11249-11270.

576

577 Hoek, E., Carranza-Torres, C.T., Corkum, B., 2002. *Hoek-Brown failure criterion - 2002 edition*. In: *Proceedings of the fifth North American rock mechanics symposium*, Toronto, Canada, vol. 1, 267-273.

578

579 Hoek, E., 2012. *Blast Damage Factor D*. Technical note for RocNews, February.

580 Hu, Y., Lu, W., Chen, M., Yan, P., Yang, J., 2014. *Comparison of Blast-Induced Damage Between Presplit and Smooth Blasting of High Rock Slope*. *Rock Mechanics and Rock Engineering* 47:1, 1307-1320.

581

582 Kim, Y., 2009. *Tunnel Contour Quality Index in a Drill & Blast Tunnel*. Norwegian University of  
583 Science and Technology. Doctoral Thesis.

584 Kim, Y., Bruland, A., 2010. *A study on the estimation of the Tunnel Contour Quality Index in a drill and blast tunnel*. *Rock fragmentation by Blasting – Sanchidrián* (ed). Taylor and Francis Group, London, 507–  
585 513.

586

587 Kim, Y., Moon, H., 2013. *Application of the guideline for overbreak control in granitic rock masses in Korean tunnels*. *Tunnelling and Underground Space Technology*; 35, 67-77

588

589 Kim, Y., Bruland, A., 2015. *A study on the establishment of Tunnel Contour Quality Index considering construction cost*. *Tunnelling and Underground Space Technology*, 50, 218-225.

590

591 Konkan Railway Corporation Ltd, 2012. *Special conditions of contract - Part - B (Tunnel)*.

592 Mahdevari, S., Haghghat, H.S., Torabi, S.R., 2013. *A dynamically approach based on SVM algorithm for prediction of tunnel convergence during excavation*. *Tunnelling and Underground Space Technology*; 38,  
593 59-68.

594

595 Mahtab, M.A., Rossler, K., Kalamaras, G.S., Grasso, P., 1997. *Assessment of geological overbreak for*  
596 *tunnel design and contractual claims*. International Journal of Rock Mechanics & Mining Sciences, 34,  
597 paper n° 185.

598 Mandal, S.K., Singh, M.M., 2009. *Evaluating extent and causes of overbreak in tunnels*. Tunnelling and  
599 Underground Space Technology, 24, 22-36.

600 Miller, J.N., Miller, J.C., 2010. *Statistic and chemometrics for analytical chemistry*. Pearson Education  
601 Limited. Edimburgh Gate. Harlow.

602 Nasserri, M.H.B., Rezanezhad, F., Young, R.P., 2011. *Analysis of fracture damage zone in anisotropic*  
603 *granitic rock using 3D X-ray CT scanning techniques*. International Journal of Fracture 168, 1-13.

604 NPRA-Norwegian Public Road Administration, 2012. *Etatsprogrammet Modernevegtunneler. Road*  
605 *Tunnel Strategy Study 1*. NPRA report no. 153.

606 NTNU, 1995. *Project Report 2A-95 TUNNELLING – Blast Design, NTNU*. Department of Civil and  
607 Transport Engineering, Trondheim.

608 Oggeri, C., Ova, G., 2004. *Quality on tunnelling: ITA-AITES Working Group 16 final report*. Tunnelling  
609 and Underground Space Technology, 19, 239-272.

610 Olsson, M., 2010. *Tunnel blast design for minimizing of the damage zone. A guidance document for SKB*  
611 *and Posiva*. Swebrec, no. 4.

612 Palmström, A., 2005. *Measurements of and Correlations between Block Size and Rock Quality*  
613 *Designation (RQD)*. Tunnels and Underground Space Technology, 20, 362-377.

614 Pelizza, S., Oggeri, C., Oreste, P., Peila, D., 1999. *Criteria for tunnel static approval test*. AFTES –  
615 Journées d'études internationales de Paris, 333-340.

616 Pelizza, S., Peila, D., Oggeri, C., 2000. *Static approval test of transportation tunnels*. Gallerie e grandi  
617 opere sotterranee, 60, 58-62.

618 Pelizza, S., Peila, D., Oggeri, C., Brino, L., 2000. *Key points for the static approval test of underground*  
619 *works*. AITES-ITA 2000 World tunnel congress, Durban, 395-398.

620 Pejić, M., 2013. *Design and optimisation of laser scanning for tunnels geometry inspection*. Tunnelling  
621 and Underground Space Technology 37, 199-206.

622 Sanchidrian, J.A., Segarra P., Lopez L., 2006. *A Practical Procedure for the Measurement of*  
623 *Fragmentation by Blasting by Image Analysis*. Rock Mechanics and Rock Engineering 39(4), 359-382

624 Scoble, M.J., Lizotte, Y.C., Paventi, M., Mohanty, B.B., 1997. *Measurement of blasting damage*. Mining  
625 Engineering, June 1997, 103-108.

626 SN - Schweizer Norm, 2004. *Conditions générales pour constructions souterraines*. SIA - Société suisse  
627 des ingénieurs et des architectes. Zurich.

628 Singh, P.K., Roy, S.K., Sinha, A., 2003. *A new blast damage index for the safety of underground coal*  
629 *mine openings*. Mining Technology, 112:2, 97-104.

630 Singh, S.P., Xavier, P., 2005. *Causes, impact and control of overbreak in underground excavations*.  
631 Tunnelling and Underground Space Technology 20, 63-71.

632 Wang, T.T., Jaw, J.J., Chang, Y.H., Jeng, F.S., 2009. *Application and validation of profile-image method*  
633 *for measuring deformation of tunnel wall*. Tunnelling and Underground Space Technology 24, 136-147.

634 Wang, T.T., Jaw, J.J., Hsu, C.H., Jeng, F.S., 2010. *Profile-image method for measuring tunnel profile -*  
635 *Improvements and procedures*. Tunnelling and Underground Space Technology 25, 78-90.

636 Xu, D.P., Feng, X.T., Chen, D.F., Zhang, C.Q., Fan, Q.X., 2017. *Constitutive representation and damage*  
637 *degree index for the layered rock mass excavation response in underground openings*. Tunnelling and  
638 Underground Space Technology 64, 133-145.

639 Yu, T.R., Vongpaisal, S., 1996. *New blasting damage criteria for underground blasting*. CIM Bulletin,  
640 vol. 89, 998, 139-145.